Continuous spectrum of a condensed discharge in a capillary

G. V. Ovechkin

V. I. Lenin Belorussian State University

Usp. Fiz. Nauk **162**, 159–179 (June 1992)

1. INTRODUCTION

When he investigated the far-ultraviolet emission of hydrogen, helium, and other gases, Lyman discovered[1,2] that a continuous spectrum (190–85 nm) was emitted by a condensed discharge in a capillary. He noted that the intensity of this spectrum was due to glass evaporation products, but was independent of gas pressure and gas composition in the discharge tube prior to breakdown.

The first publication devoted to the emission of a continuous spectrum by a condensed discharge in a narrow tube with a diameter up to 1 cm is due to Anderson.[3] The discharge was slowly decaying. Anderson determined both the resultant emission and the emission in each half-period of the discharge. At high voltages, the discharge produced a continuous spectrum with the emission and absorption lines of silicon atoms and ions superimposed upon it. According to Anderson's experimental data, the emission was of thermal origin. He estimated that the plasma temperature in the spark channel was 19 000 to 50 000 K.

Rathenau[4] used the continuous spectrum emitted by a condensed discharge in a capillary to examine the absorption spectrum of water vapor and gaseous carbon dioxide below 200 nm. He considered that the continuous emission down to 50 nm was of thermal origin, and ascribed emission below this limit to bremsstrahlung.

Gasilevich[5] noted that the intensity of the continuous spectrum was different for discharges produced in capillaries made of different types of glass.

The presence of emission and absorption lines in the continuous emission spectrum of the plasma in a condensed discharge in a capillary led Finkelnburg[6–8] to the conclusion that the lines are emitted and absorbed by atoms and ions inside the capillary channel. The continuum is then entirely due to bremsstrahlung by electrons in fields produced by ions and to recombination between them. He ascribed the line broadening associated with higher plasma pressures to the Stark effect.[8]

In addition to studies of emission by discharges in capillaries and narrow tubes, there are also investigations of the continuous spectrum emitted by other sources. Thus, Wyneken[9] examined spark discharges under water and found that there was both a line spectrum and a strong continuous emission of roughly equal intensity in the wavelength range 240–650 nm. Elenbaas[10–12] determined the emission intensity of a high-pressure mercury lamp for a number of wavelengths between emission lines. Unsöld[13] used these data to construct the energy distribution in the spectrum. The intensity of the mercury lamp is almost constant across the wavelength range 230–530 nm. It rises markedly only in a small interval at longer wavelengths.

In accordance with these experimental data, Unsöld[13] used the following procedure to derive a formula for the emission of a gas per unit frequency per unit volume. According to the Kramers formula,[14,15] the absorption coefficient of a single hydrogen-like atom in the nth quantum state is

$$a_n = (1/n^2)(64\pi^4/3\sqrt{3})(me^{10}/ch^6n^3)/\nu^3 . \tag{1.1}$$

The ratio of the number of atoms in state n to the number in the ground state $n = 1$ at temperature T is given by the Boltzmann expression

$$n^2\exp[-(E_1 - E_n)/kT],$$

where $E_n = Rhc/n^2$ is the energy of the nth quantum state and n^2 is the statistical weight of this state relative to the ground state. For the sake of brevity, we shall use the notation $U_n = E_n/kT = (Rch/kT)/n^2$ and

$$U = h\nu/kT. \tag{1.2}$$

The bound-free part of the resultant absorption coefficient per ground-state atom is given by

$$\varkappa_\nu = (64\pi^4/3\sqrt{3})(me^{10}/ch^6\nu^3) \times \sum_{h\nu/kT > U_n} (1/n^3)\exp[-(U_1 - U_n)]. \tag{1.3}$$

To extend these calculations to other atoms, we must correct (1.3) by using the following quantities: (1) the effective atomic number $Z_{\rm eff}$ of the atomic residue, (2) the statistical weight of the ground state γ, and (3) in complex spectra consisting of many series of spectral lines, the sum in (1.3) can be replaced with the integral

$$\sum(\Delta n/n^3)\exp[-(U_1 - U_n)] \to (1/2)\int \exp[-(U_1 - U_n)]d(1/n^2)$$
$$= -(\exp(-U_1)/(2U_1)\int_U^0 \exp U_n dU_n = [\exp(-U_1)/2U_1](e^U - 1) . \tag{1.4}$$

Consequently, for the portion of the absorption coefficient that is due to the bound-free transitions, we have (per atom)

$$\varkappa_\nu = (\gamma\cdot 1.6\pi^2/3\sqrt{3})\left(e^6Z_{\rm eff}^2/chk^2\right)[\exp(-U_1)/T^2]\frac{e^U - 1}{U^3}, \tag{1.5}$$

where U is the actual ionization energy of an atom, divided by kT.

 0038-5670/92/060520-11$03.00

To allow for the absorption coefficient in the region of free-free transitions of electrons outside the atom, we must integrate (1.4) between $U=0$ and $U=-\infty$, so that instead of the factor $e^U=-1$ in (1.5) we obtain 1.

If in addition to bound-free transitions we include free-free transitions, then the factor e^U-1 in (1.5) is replaced simply with e^U.

At high gas pressures, there is a further contribution due to continuous absorption caused by electron transitions involving strongly broadened states below the true ionization limit. This continuous sequence of atomic energy states will be denoted by $\Delta U=\Delta E/kT$ with negative energy value. Integration of (4) must then be carried out between $U=U+\Delta U$ and $U=-\infty$. The result of this is that the factor e^U in (5) is replaced with $e^{U+\Delta U}$ or, for electrons bound to the nucleus, by the factor $e^{U+\Delta U}-e^U$.

The final expression for continuous absorption by partially ionized gas then becomes (per atom)

$$\varkappa_\nu=(\gamma\cdot 1.6\pi^3/3\sqrt{3})(e^6Z_{\rm eff}^2/chk^3)\left(\exp(-U)/T^2\right)(1/U^3)e^{U+\Delta U}. \tag{1.6}$$

The absorption coefficient consists of three parts, namely, free-free, free-bound, and bound-bound broadened lines in the ratio of

$$1,\quad e^U-1,\quad e^{\Delta U+U}-e^U, \tag{1.7a}$$

or

$$e^{-U},\quad 1-e^{-U},\quad e^{\Delta U}-1. \tag{1.7b}$$

An important conclusion follows from these ratios. When the temperature of the arc discharge is $T=6000$ K and $U=1.43/\lambda T$, we obtain $U=6$ and $e^{-6}\ll 1$ for $\lambda=400$ nm, i.e., there is no absorption due to electron transitions in the region of the broadened lines. For discharges in which $\Delta U>1$, the dominant absorption process is due to transitions of bound electrons.

In laboratory practice, it is convenient to define the intensity emitted per unit frequency in a solid angle of 4π, i.e., $4\pi\varepsilon_\nu$. We therefore transform from the absorption coefficient per atom to the absorption coefficient per unit volume, which we can do by multiplying $\varkappa_\nu$ in (6) by the number of atoms per unit volume, i.e., $n=P_g/kT$, where P_g is the gas pressure.

Absorption of light is usually accompanied by spontaneous and stimulated emission. In steady-state processes, the total radiated power must be equal to the total absorbed power. Unsöld took into account the Wien part of the Planck function, namely,

$$\rho(\nu_{kl})=(8\pi h\nu^3/c^2)\exp(-U).$$

In accordance with (6), the resultant emission per unit volume per unit frequency is found to be

$$4\pi\varepsilon_\nu=(\gamma\cdot 1.28\pi^3/3\sqrt{3})(e^2/h\nu)^3Z_{\rm eff}\exp[-(U_1-\Delta U)]P_g. \tag{1.8}$$

This expression does not contain the frequency, but it was not explained why the derivation of the formula was based on the assumption of thermodynamic equilibrium for radiative processes, whereas the radiant energy obtained by solving the problem turned out to be frequency-independent in the spectral range defined by $h\nu\lesssim E_1$.

Babushkin[16–20] published a number of papers on the nature of the emission spectrum produced by condensed discharges in narrow glass or quartz tubes. He produced the spectra by discharging capacitors of 0.25–1.0 μF at 30–60 keV. The discharges were initiated between pointed aluminum electrodes in a tube of 0.25–6 mm in diameter. The electrode separation was 3–4 cm. The discharges were slowly decaying. In rapidly decaying discharges, the continuous spectrum was found to be stronger. Babushkin determined the spectral composition of the resultant emission and the emission in each half-period of the discharge. He found that there were broad spectral lines superimposed on the continuum.

Babushkin was the first to introduce different metals into the tube channel. He found that the emitted intensity was different for different metals. He tried to explain the increase in intensity in terms of an increase in the number of electrons with decreasing atomic ionization energy. However, this was not confirmed by experiment.

He then cut an aperture (nozzle) in the wall of the tube[18] and used a rotating mirror to determine the rate of outflow of evaporation products in the radial direction. He was able to calculate the pressure in the tube from the ratio of shock-wave velocity and pressure behind the wavefront[21] for breakdown voltages of 30, 43, and 60 kV. This pressure was found to be 13, 14, and 21 atm, respectively. He then used these data together with a set of equations that included the Saha equation[22] to calculate the plasma temperature and degree of ionization in the tube channel.

Babushkin[20] determined the radiant intensity of the discharge by observing it with the tube end-on and side-on. The two intensities were found to be the same despite the tenfold difference in the thickness of the radiating plasma, which is in agreement with Ref. 3.

His measurements led Babushkin to the conclusion that the radiation emitted by the condensed discharge in a narrow tube had thermodynamic and equilibrium character.

The controversy about the nature of the radiation from a condensed discharge in a capillary has continued. Hahn and Finkelnburg[23] made direct photocell measurements of the radiant intensity of condensed discharges in a capillary for a number of wavelength groups. The intensity was found to be constant between 650 and 400 nm, which is in agreement with Unsöld's formula (8). However, the intensity was much lower at shorter wavelengths. Hahn and Finkelnburg showed that there was a linear relation between the intensity and the square of maximum current density in the capillary discharge. They then used this result and the presence of spectral lines in the continuum to conclude that the intensity of the continuous spectrum produced by a condensed discharge in a capillary was proportional to the number of collisions between electrons and positive ions. On this basis, they again came to the conclusion that the continuous spectrum was due to bremsstrahlung. On the other hand, the fall in intensity at shorter wavelengths was explained as being mostly due to recombinations between electrons and ions. This explanation is in conflict with Unsöld's conclusion expressed by (7). The continuum of energy states ΔE was totally ignored in this interpretation.

In a later paper, Finkelnburg[24] associated the emission

of the continuous spectrum and the spectral lines with thermodynamic equilibrium; he ascribed absorption lines to a departure from thermodynamic equilibrium in the plasma.

Other workers[25-27] photographed the emission spectra of condensed discharges in capillaries and found that the intensity was constant within the range 400–300 nm, and then fell at shorter wavelengths. According to Unsöld, the transition from constant to variable intensity should depend on the ionization energy of the main element. Observations[25-27] showed that the intensity was different for different gases (and for capillaries made from different materials) at relatively low current densities, but the above shift of the transition between the two regions was not detected.

Romand and Vodar[27] showed that discharges in silica capillaries (melting point 1400 °C, boiling point 2230 °C) emitted a bright continuous spectrum at relatively low current densities. Discharges in a zirconium capillary (melting point 2700 °C, boiling point 4300 °C) emitted a weak continuum even at high current densities, but this was not explained.

Spectral lines are well defined against the continuum in all the above experiments with discharges in capillaries. Finkelnburg and, later, Biberman decided on this basis that the continuous spectrum can only be due to bremsstrahlung emitted by electrons in the field of ions, and to electron-ion recombinations. According to Biberman and Norman,[28] 'the electron can be in a bound state (its energy is then negative and assumes discrete values) or in a free state (in which its energy is positive and can vary continuously)'. The continuous spectrum is due to transitions of electrons from free to bound states (free-bound transitions) or to free-free transitions. Calculations[28] show that, for any atom, the ratio of these components of the continuum for $\nu < \nu_g$ is approximately $(e-1):1$. The contribution of free-bound transitions predominates when $h\nu < 0.7kT$. When $h\nu > 0.7kT$, free-free transitions predominate across the frequency range up to the thresholds for particular levels. This excludes the possibility that a continuous series of energy states is formed in atoms and ions, so that the ratio of the corresponding contributions to the continuum is different from the Unsöld case indicated by (7).

The theoretical conclusions of Biberman and Norman[28] can be summarized by the following formulas for the emitted intensity:

$$\varepsilon(\nu,T) = C_4(2\Sigma_1/\Sigma_0)\exp[-U_1 + (h\Delta\nu/kT)]Z^2\xi(\nu)kTN_a \text{ for } \nu \leqslant \nu_g, \tag{1.9}$$

$$= \varepsilon(\nu_g, T)\xi^{-1}(\nu_g)\exp(U_g - U) + \sum \varepsilon_{nl}(\nu, T) \text{ for } \nu > \nu_g, \tag{1.10}$$

where

$$C_4 = 32\pi^2 e^6(3\sqrt{3}h^3c^3)^{-1} = 0{,}95\cdot 10^{-7}.$$

The quantity $\varepsilon(\nu,T)$ refers to a thickness of 1 cm and is given in units of $\text{erg}\cdot\text{s}^{-1}\text{cm}^{-1}\text{sr}^{-1}(\text{s}^{-1})^{-1}$.

In the experiments described above the discharge was produced in tubes or capillaries made of inorganic materials such as different types of glass, quartz, ceramics, porcelain, and so on. It was noted that the emitted intensity was low and depended on the melting point of these materials. A capillary made of a readily evaporated material was used in Refs. 29–31 to increase the density of the radiating plasma during the discharge. Four capacitors with a total capacitance of 100 μF, charged to 3 kV, were used in Ref. 29 to produce a discharge in a capillary in a textolite plate 2 mm in diameter and 10 mm long. The duration of the discharge was approximately 100–400 μs when the inductance in the discharge circuit was 1.5 μH. The current density was up to 4×10^5 A/cm^2. The plasma was in thermodynamic equilibrium at a temperature of 39 000 K and pressures of 500 and 120 atm. The plasma radiation was found to correspond to a black body at this temperature.[30]

A plasma flare was found to issue from the capillary. Its length was in excess of 100 mm and its diameter was 15 mm. The flare emitted a continuous spectrum as well as lines due to the ions CII, CIII, and OII. "The flare was surrounded by a plasma layer, 40 mm thick, at a lower temperature. It emitted CI, MgI, CaI lines as well as CN molecular bands" (Ref. 31). Moreover, "... the flare leaving the capillary was surrounded over a length of about 3 mm by a partially opaque ring with inner and outer diameters of about 2 and 6 mm.... The temperature of the opaque layer was relatively high, since its emission contained lines due to CII, and CIII. The continuous spectrum was almost totally absent. The presence of fine particles at such high temperatures can be explained in this case by the fact that, owing to the high rates of flow, the particles traversed a distance of 2–3 mm in a very short time that was too short for them to evaporate" (Ref. 31). Consequently, it seems to us that the radiation from the plasma in the capillary channel propagates through this ring and flare, which means that the internal emission is attenuated and removed by self-absorption and self-inversion, and is augmented by spectral lines.

Experiments[29,30] have shown that the emission due to the discharge produced in the textolite capillary was of thermal origin. Other experiments[31] confirmed that the energy distribution in the continuous spectrum between lines was in agreement with the Biberman theory and formulas. On this basis, the final conclusion is that the continuous spectrum is entirely due to bremsstrahlung by electrons in the field of atoms, and to electron-ion recombinations.

The authors of Ref. 33 reported that the intensity distribution in the spectrum was in agreement with the Unsöld theory but not with the Biberman-Norman theory.

2. THE CONDITIONS FOR AND THE PLACE OF FORMATION OF THE CONTINUOUS SPECTRUM AND THE SPECTRAL LINES

Even under optimum discharge conditions, the experiments described above record continuous spectra with spectral lines superimposed upon them. This has led to the suggestion[23,24,28] that the spectral lines are emitted at the same time as the continuum, the latter being entirely due to bremsstrahlung and recombinations. According to Ref. 28, a bound electron is in a rigorously discrete state of an atom or ion, whereas Unsöld[13] and Inglis and Teller[32] admit that the energy states can become perturbed and may overlap, which results in the appearance of a continuum of atomic and ionic upper energy states. The experimental problem is to elucidate the possibility of this continuum and to determine its

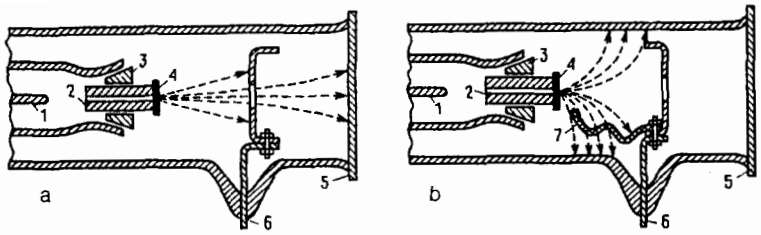

FIG. 1. Configuration of the end of the discharge tube: *1*—internal electrode, *2*—fused-quartz capillary, *3*—Plexiglass plug, *4*—aluminum ring slipped on to the end of the capillary, *5*—quartz window, *6*—external electrode, *7*—bent metal plate.

depth. However, the first step must be to establish whether a pure continuum is indeed emitted from the center of the capillary channel, and to identify the point at which the spectral lines originate.

We therefore constructed a discharge tube[34,35] that was transparent on all sides and contained a capillary mounted with the help of Plexiglass end plates and Picein. A quartz capillary, 6 cm long and 1.5 mm in diameter, with walls 2–3 mm thick, was used for visible and ultraviolet radiation. The radiation emitted by the discharge was observed through crystalline quartz windows attached to the capillary at the end and at the sides of the discharge tube. A narrow aluminum ring was slipped on the end of the capillary to separate the emission of the flare from the internal emission. The shape, disposition, and orientation of the external electrode have the very important function of protecting the end window from contamination by evaporation products arriving from capillary walls. When the electrode is located and oriented as shown in Fig. 1a (Ref. 35), the window becomes contaminated after only one discharge. However, when the shape, disposition and orientation of the electrode is as in Fig. 1b, the window remains clear after any number of discharges.

The temperature of the capillary was determined from the afterglow and thermoluminescence of fused quartz.[34,36]

The source of radiation was a discharge produced by a capacitor of 0.6 or 0.7 μF, with connector resistance of 0.5 Ω (Ref. 35). The inductance of the discharge circuit was 1.1 μH. A resistance of 1.0 Ω appears in the capillary channel when the discharge is initiated. The air pressure in the discharge tube prior to the end of the discharge is about 0.01 Torr. The voltage across the capacitor was determined from the breakdown voltage between two spherical electrodes (diameter 10 mm) in the discharge circuit.

Figure 2 shows the current oscillogram for the circuit without the discharger, recorded with a Rogowski belt across a resistor.[36] The current oscillations are seen to be lightly damped.

Figure 3 shows the current oscillogram recorded by discharging a capacitor of 0.6 μF with 16 kV across it. It is clear that the current oscillations are highly damped, and cease altogether after about 10 μs. A 1.0-μF capacitor discharges in this circuit in three or four periods (15 μs).

The current density during the first half-period of the discharge was of the order of 10^6 A/cm^2.

The radiant intensity of the discharge has often been reported in the literature as depending on the composition of the evaporating material. We have shown[35] that the intensity depends on the physical properties of the material as follows.

Since, according to Unsöld's formula (1.8), the emitted energy is the same at all frequencies in the visible and ultraviolet ranges, and is proportional to the plasma pressure, the relative intensity of the discharge in the capillary was measured with an oxygen-activated cesium photocell and an electrometer, using the circuits described in Ref. 23. The photocell was illuminated without using a condenser, and the results were reported in Ref. 36. These data were used to construct the relative intensity of the discharge in the capillary as a function of the boiling point of the materials used (Fig. 4).[37] It is clear from the graph that the radiant intensity of the discharge is a definite function of the boiling point of the evaporated material. According to Trouton's rule, the heat of evaporation of simple materials is directly proportional to the boiling point. Consequently, both the amount of material evaporated during the short period of the capacitor discharge and the plasma pressure increase with decreasing heat of evaporation, i.e., with decreasing boiling point.

On the other hand, the radiant intensity is found to be proportional to the plasma pressure.

To elucidate the origin of the continuous spectrum, the plasma emission was photographed from the end of the tube,

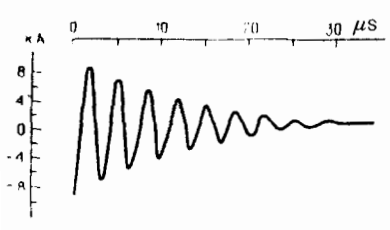

FIG. 2. Oscillogram obtained by discharging a capacitance of 0.5 μF at 16 kV between discharge spheres without the discharge tube.

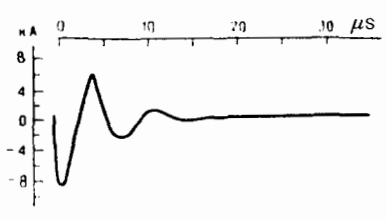

FIG. 3. Oscillograms obtained by discharging a capacitance of 0.5 μF at breakdown voltage of 16 kV across a discharge tube and the spherical discharge terminals connected in series.

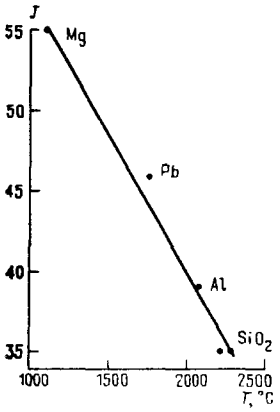

FIG. 4. Emission intensity as a function of the boiling point of the material on the surface of the capillary channel at constant maximum current density in a pulsed discharge.

without a condenser, under different discharge conditions. We note that, in the vacuum ultraviolet, the absorption spectra were photographed without using a condenser.[4] The capillary axis was then strictly aligned with the optical axis of the spectrograph.

An arrangement of four vacuum-tube rectifiers, commonly used in x-ray practice and producing a continuous current through the discharge tube, was employed. Only the molecular spectrum of nitrogen was emitted during the gas discharge in the capillary.

The spectrum emitted by the quartz capillary during pulsed discharges of the capacitor charged to 4 kV was found to consists of molecular bands and lines due to the components of the atmosphere. A line spectrum consisting mostly of atmospheric atomic lines was emitted by condensed discharges in a quartz capillary for a breakdown of 5 kV. Molecular bands were then absent, indicating that the molecules were completely dissociated.

For breakdown voltages above 5 kV, a line spectrum was again emitted, the strongest lines being due to silicon atoms and ions, and there was also a continuous background. This background was mostly due to electron-ion recombinations.

The lines due to silicon and oxygen atoms and ions become very broad as the breakdown voltage increases, and this is accompanied by a reduction in the intensity of the strongest lines and an increase in the background intensity.

Finally, for the electrode arrangement shown in Fig. 1b, held at a certain voltage, a continuous spectrum is emitted with SiI, SiII, SiIII, and SiIV emission lines superimposed upon it. The intensity of these lines is not very different from that of the continuum. There are no absorption lines. When the external electrode is arranged as shown in Fig. 1a, there are appreciable absorption lines in addition to the silicon lines in the range 250.6–252.8 and, especially, the SiI 288.1 nm line. The Doppler effect was used to determine the velocity of the plasma issuing from the capillary by recording the shift of the 288.1-nm line. The magnitude of this velocity was found to be 60 ± 20 km/s. The large uncertainty of this result was due to possible overlap effects.[38]

A condenser is essential when one investigates visible and ultraviolet emissions. In the case of a capillary with opaque walls, the emission from the end of the capillary and the emission of the flare are projected by a condenser onto the spectrograph slit.

We used a long quartz capillary that was transparent to visible and ultraviolet radiation. The highest intensity on the photographic emulsion is then obtained by photographing the spectrum from the end of the tube and using a condenser to focus the radiation from the interior of the capillary on the spectrograph slit. When the external electrode has the shape and orientation shown in Fig. 1b, the radiation emitted by plasma outside the capillary is almost entirely excluded. Figure 5 shows scans of the spectra photographed in this way. The spectra were recorded with $\times 3$ linear magnification.

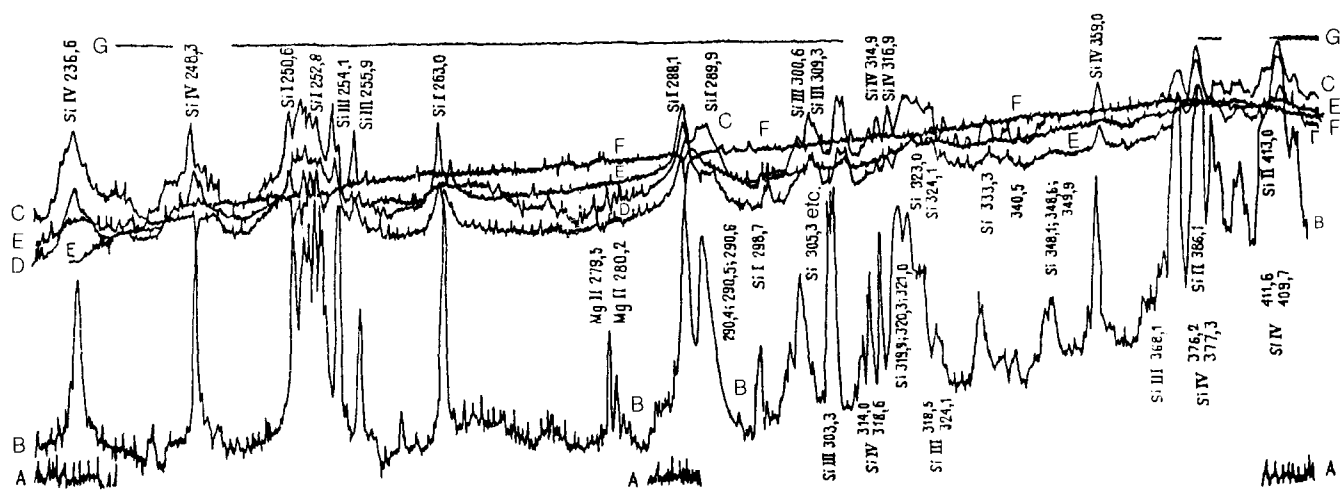

FIG. 5. Emission spectra recorded in the interior of the quartz capillary, photographed from the end of the discharge tube for different breakdown voltages. B—after fifteen discharges at breakdown voltage of 6 kV, C—after six discharges at 9 kV, D—after three discharges at 12 kV, E—after two discharges at 14 kV, F—after one discharge at 16 kV, using a reduced gap width.

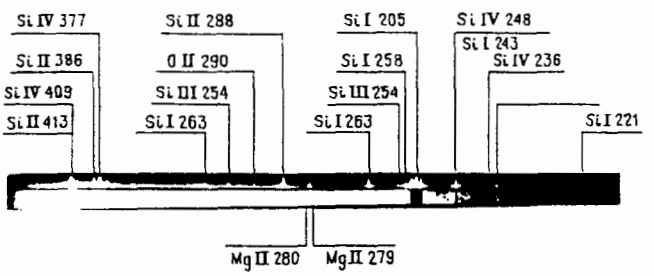

FIG. 6. Emission spectrum recorded from the end of the capillary. The spectrum was photographed from the side of the tube with the capillary parallel to the slit of the quartz spectrograph and the image of the capillary focused by a condenser on the spectrograph slit.

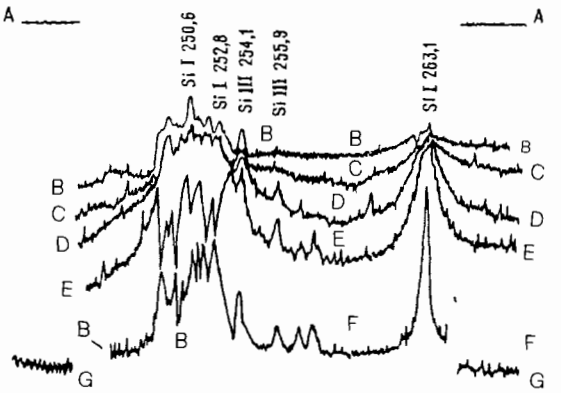

FIG. 7. Microphotograms obtained at different heights on the spectrum shown in Fig. 6. B, C—plasma emission spectra at 3 and 1 mm from the end of the capillary in the interior of the channel, D, E, F microphotograms recorded at distances of 0.3, 1.5, and 2.5 mm from the end of the capillary.

They clearly show that the intensity of all the lines decreases whereas the intensity of the continuous radiation increases with increasing breakdown voltage. Line broadening gradually transforms the line spectrum into a pure continuum.

For low current densities, the continuous background behind the line spectrum is largely due to electron-ion recombinations, as predicted by Unsöld's theory[13] and confirmed experimentally in Refs. 33 and 39.

An increase in breakdown voltage is accompanied by an increase in the current density in the pulsed discharge, and by an increase in the temperature and plasma density in the capillary channel. This enhances the interaction between the plasma components and the perturbation of excited atomic and ionic states, which in turn leads to higher continuum intensity. For a breakdown voltage $\geqslant 16$ kV, the current density reaches 10^6 A/cm^2. The result of this is a very high temperature in the capillary and a very high pressure in the plasma consisting of the evaporation products from the capillary walls, which produce such a great increase in the interaction between the plasma components that the concept of atomic and ionic energy levels ceases to be meaningful for some or all the excited states.

Finkelnburg[8,23,24] and Biberman[28] maintain that the continuous spectrum is mostly due to bremsstrahlung by electrons with the simultaneous emission of spectral lines that are swamped by continuous emission. These conclusions do not agree with the experimental data. The spectra of Figs. 6 and 7 clearly show sharp images of resonance lines of the manganese ion, due to transitions of electrons from an unperturbed energy level to the ground states. These states lie below the continuous sequence of energy levels (see Table I). It is clear from the obtained spectrum that the lines are not swamped, but are well-defined against the background continuum.

TABLE I. Results calculated from (4.1) and (4.2) and tabulated data from Refs. 43, 44.

№	Atom or ion	Ionization energy E_i, eV	$E - E_1$, eV	Effective ionization energy E_1, eV		$\Delta E = E_1 - E_l$, eV	Calculated energy E_l below which discrete states remain		Resonance line				Lines whose broadening can be seen in the visible and ultraviolet			
									emitted from level	vanishes	persists	in vacuum range	λ from level		λ from level near E_1	
				eV	cm^{-1}		eV	cm^{-1}	cm^{-1}	nm	nm	nm	nm	cm^{-1}	nm	cm^{-1}
1	MgI	7,64	1,89	5,75	46 380	0,81	4,94	39 846	35 051	235,2						
2						1,42	4,33	34 925								
3	MgII	15,03	3,0	12,03	97 034	2,93	9,10	73 401	35 730		279					
4						5,13	6,90	55 655			280					
5	SiI	8,15	1,89	6,26	50 493	0,88	5,38	43 395	39 760	251,4			288,1	40 992		
6						1,54	4,72	38 072								
7	SiII	16,34	3,0	13,34	107 600	3,55	9,79	78 966	55 310			180	385	81 252	413	103 556
8						6,21	7,13	57 511	76 666			130	635,5	81 232	505	101 025
9	SiIII	33,46	3,92	29,54	238 270	8,69	20,55	165 576	82 881			120,6	254	122 215	304	234 442
10						15,21	14,33	115 586								
11	SiIV	45,13	4,75	40,38	325 705	17,13	23,25	268 295	71 595			139,7	409,7	218 375	237	318 743
12						29,98	10,40	83 886							324	322 338
13	OI	13,61	1,89	11,72	94 533	1,64	10,08	87 113	76 795			130			777	86 629
14						2,87	8,85	71 384								
15	OII	35,11	3,0	32,11	256 098	7,92	24,19	195 117	119 933			83,38	465	206 895	429,3	255 794
16						13,86	18,25	147 205							460	256 139
17	OIII	54,89	3,92	50,97	411 124	17,20	33,77	272 389	120 059			83,29	376,2	294 077	373	401 510
18						30,10	20,87	168 337							364	405 851

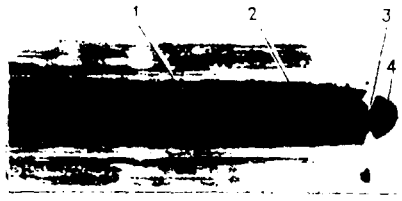

FIG. 8. Photograph of the end of the quartz capillary recorded side-on: *1*—capillary walls, *2*—emission inside the capillary, *3*—metal ring slipped on the end of the capillary to mark its end, *4*—emission by the flare.

A narrow aluminum ring was slipped on to the capillary in order to display more clearly the presence of the flare. The radiation from the discharge in the capillary was photographed side-on for a breakdown voltage of 14 kV (Fig. 8). The photograph clearly shows that the condensed discharge is accompanied by a bright emission not only from the interior of the capillary (region 2), but also from outside the capillary (region 4). However, the photograph distorts the size of the channel diameter relative to the diameter of the entire thickness of the capillary. On the photograph, the channel diameter is equal to almost half the diameter of the capillary. This can probably be explained by the ability of the capillary walls to magnify the image by analogy with a lens. In reality, the channel diameter is only one quarter of the total thickness of the capillary.

To determine the spectral composition of the plasma emission at different points along the capillary axis, and outside the capillary, the spectra were photographed in the following way. The capillary was mounted parallel to the spectrograph slit, and the emission from the channel at the end of the capillary and outside was focused on the spectrograph slit. The image of the source on the spectrograph slit was produced by a condenser in such a way that the illumination of the slit was exactly the same as if the source was on the slit. The radiation emitted by each point on the slit then simulates the plasma emission at different points in the capillary channel and outside the channel along the axis. Figure 6 shows the spectrum produced by a single discharge for a breakdown voltage of 15 kV. The quartz spectrograph did not magnify the image. It is clear from the spectrum that the spectral lines originate from outside the capillary, whereas the continuous spectrum is emitted from its interior. It is also intensively emitted outside the capillary over a length of approximately 0.5 mm. Inside the capillary, the continuous spectrum contains narrow atomic absorption lines due to silicon. Figure 7 reproduces the tracings obtained for this spectrum between the SiI 263.1 and SiIII 2.54.1 nm lines. The tracings of Fig. 9 were obtained in a similar way for the spectrum photographed in a low-dispersion glass spectrograph at wavelengths between 380 and 480 nm.

It is clear from the tracings of Fig. 7 that the 263.1-nm emission line is only just noticeable above the continuous spectrum of the plasma at 3 mm inside the capillary from its end. The line wings fall off very slowly and are quite spread out. The line profile becomes better defined as the radiating plasma approaches the end of the capillary and as it departs from this end. It is also clear that the lines emitted from the interior of the capillary broaden until they vanish altogether. Absorption occurs only at the central part of the atomic emission line. Consequently, the temperature of the absorbing vapor is several times lower than the plasma radiation temperature. This suggests that a thin layer of vapor is present between the plasma and the capillary wall. The composition of this layer varies rapidly because it is continuously replenished by evaporation from the capillary walls and, at the same time, its vapor continuously diffuses into the plasma. Vapor passing through this layer can be dissociated, excited, ionized, and even heated by absorption.

Next, it is clear from Fig. 7 that the group of silicon atomic lines lying between 250.6 and 252.8 nm in the capillary channel, where the plasma is surrounded by the vapor layer due to the wall evaporation products, is seen in absorption. As soon as the plasma leaves this environment, the lines can be seen in emission. Their intensity is greater than the continuum intensity inside the capillary. The line intensity persists to a distance of 1.5 mm from the capillary, which is probably explained by an increase in the number of neutral atoms due to electron-ion recombinations outside the capillary. Consequently, outside the capillary, the continuous emission is largely due to electron-ion recombinations.

It is also clear from these tracings that the SiIII lines between 254.1 and 255.9 nm are broadened in the interior of the channel until they merge with the continuum. Outside the capillary, their intensity exceeds the continuum intensity

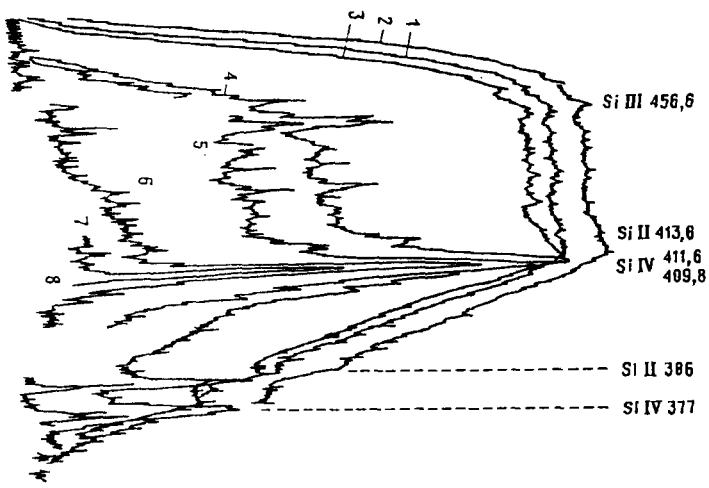

FIG. 9. Microphotograms recorded at different heights of the spectrum, obtained with a glass spectrograph in the same way as the spectrum in Fig. 6. *1–3*—internal plasma emission spectra at 4, 2.5, and 1 mm from the end of the capillary, *4–8*—plasma emission spectra recorded at 0, 2, 3, 4 and 4.5 mm from the end of the capillary.

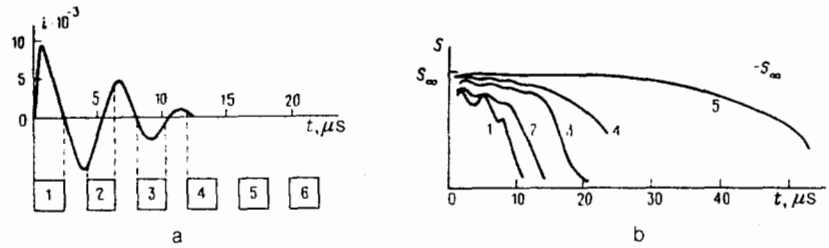

FIG. 10. a—Current oscillogram recorded by discharging a 0.6-μF capacitor at 25 kV (the time intervals at which the spectra were photographed are indicated under the curve); *1–6*—running numbers, b—Time-resolved resultant plasma emission from the capillary channel, recorded by the SFR-2 camera for different voltages across the capacitance (*1*—7 kV, *2*—10 kV, *3*—14 kV, *5*—15 kV); *1–3*—continuous photography with photorecorder slit of 0.3 mm, *5*—without slit, *4*—frame by frame. S_∞ is the blackening obtained with the microphotometer photocell covered.

inside the capillary. The intensity of the 254.1-nm line at 0.3 mm from the end of the capillary is higher than the intensity of the continuum inside the capillary. This can probably be explained by an increase in the number of the doubly-ionized silicon atoms due to recombinations between electrons and triply-ionized silicon atoms, which ensures strong continuous emission by the plasma at a distance from the capillary.

Figure 9 shows tracings obtained for the SiIII lines at 455.2, 456.6, and 457.4 nm and the SiIV lines at 409.7, 411.6, and SiII 413.0 nm. The spectra show that the continuous spectrum originating in the capillary channel is free of emission lines. The radiation emitted by the plasma near the end of the capillary contains only traces of the broadened lines. Outside the capillary, emission lines are found to emerge rapidly from the continuum. As the plasma flows through the capillary, triply-ionized silicon atoms disappear as a result of recombinations with electrons. Hence, only the single 413.0-nm line of SiII remains as the plasma departs from the capillary to a distance of 0.5 mm, and its emission intensity is comparable with that of the continuum at the end of the capillary channel. As the plasma departs from the capillary, its line emission intensity is found to decline slowly, but the intensity of the continuum falls rapidly. At the same time, there is a rapid reduction in the line width.

The energy of the flare is replenished by absorption of radiation from the capillary channel. The flare tends to reduce rather than increase the emission intensity from the channel.

It is clear from the foregoing that, under optimum discharge conditions, the interior of the capillary emits a line-free continuum. The line spectrum originates in the flare outside the capillary. Absorption lines are produced on the periphery of the capillary walls. These experimental data confirm that the continuous spectrum gradually transforms into a line spectrum outside the capillary.

3. PLASMA EMISSION SPECTRUM DURING A DISCHARGE

To follow the evolution of the discharge, the outflow of plasma, and its spectral composition, we examined the state of the discharge at each instant of time (with a resolution of 10^{-8} s), using the SFR-2 rotating-mirror system as a photorecorder and a time-lapse camera with beam speed of 3 km/s (Ref. 35).

The plasma inside the capillary was quasineutral. However, outside the capillary, the electric field had a definite effect on the motion of the ions. The rotating-mirror system was used to show that the plasma leaving the capillary channel in the direction of the cathode split into a number of beams which could be identified with sufficient precision as SiI, SiII, SiIII, and SiIV. The outflow velocities were 10 ± 2, 20 ± 3, 30 ± 3, 30 ± 4, and 40 ± 6 km/s, respectively. Oxygen is a component of these flows.

It was shown in Ref. 35 that the plasma temperature was $(5 \pm 1) \times 10^4$ K).

The outflow of plasma toward the anode was more uniform as compared with the beam propagating toward the cathode, and its velocity was 50 ± 20 km/s, which was in agreement with the result obtained from the shift of the silicon lines.[38] The velocity was somewhat higher when the residual-gas pressure in the tube prior to discharge was 0.008 Torr than it was at 0.1 Torr.

The SFR-2 was used as a photorecorder to photograph the intensity of the resultant emission of the discharge as a function of time for different breakdown voltages. Figure 10b shows the time-resolved resultant emission obtained in this way. It is clear from these data that, for voltages in excess of 15 keV, the emission not only does not vanish when the current passes through zero, but is only slightly attenuated, indicating that the heat capacity of the long thin-walled quartz capillary is high. Comparison of the curves of Figs. 10a and 10b shows that the plasma exhibits persistent afterglow. The duration of this is several times longer than the capacitor discharge time, which is probably due to both good thermal insulation of the capillary and the processes occurring in the plasma, namely, electron-ion recombination, the decay of perturbations of energy states, and the transfer of energy by absorption and inelastic collisions of the second kind.

To elucidate its spectral composition, the radiation was photographed at different times, using a low-dispersion glass

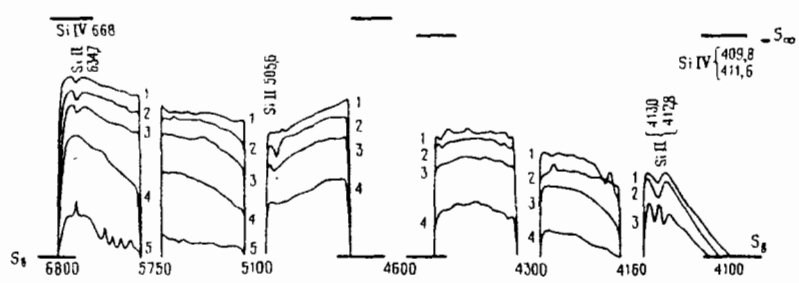

FIG. 11. Microphotograms of successive frames. *1–5*—frame number. S_f — fog, S_∞ —blackening with photocell covered.

spectrograph and the SFR-2 as a time-lapse camera. The time intervals at which the successive frames were exposed are indicated on the oscillogram of Fig. 10a. The frame exposure time was 2.3 μs. We note, first of all, that the last two frames were exposed after the discharge was over. The wavelengths covered by each frame are indicated at the bottom of Fig. 11 and the frame numbers are shown on the right. We also note that the intensity of the emission produced by the discharge between 410 and 418 nm is highly attenuated by absorption in the detector optics.

It is clear from the tracings of Fig. 11 that the spectrum recorded in the first four frames is continuous and free from emission lines, whereas the fifth frame shows a line spectrum with broadened emission lines and strong continuous background. The sixth frame shows narrow lines without a background. Next, it is clear that an intense continuous spectrum is emitted throughout the condenser discharge and even after the current stops. The fourth frame was photographed after the capacitor discharge was virtually over. Here again there are no emission lines and a transition from the continuum to the line spectrum is only just beginning and is not complete until frame 6. It is also clear that, while the capacitor was discharging, i.e., on the first three frames, there are very broad absorption lines in the region of SiIV 409.8 and 411.6 nm and SiIV 666.7, 668.0, and 670.1 nm. These absorption lines are unresolved in the low-dispersion spectrogram and are therefore seen as two very broad features. Frame 2 shows the broad SiII 505.6-nm absorption line. Its intensity is compensated in the resultant emission of the discharge and is therefore not observed in the continuous spectrum of the entire discharge.

According to the theory of Finkelnburg[8,23,24] and Biberman,[28] the emission spectrum of the condensed discharge in a capillary is largely due to electron bremsstrahlung and electron-ion recombinations. The electrons participate in two forms of motion, namely, random thermal motion and directed motion in the electric field. The probability of bremsstrahlung by a directed beam of electrons should be enormous as compared with thermal motion. The intensity of the continuum should then be very sensitive to the approach of the current to zero and, even more so, to its passage through zero, when only the thermal motion of the electrons remains. However, it is clear from frames 1–3 that this is not in fact observed. All that happens is that the intensity of the continuum gradually falls as a function of time during the discharge. In view of this, we may conclude that the continuous spectrum emitted in the above spectral range by a condensed discharge in a capillary is mostly due to transitions of bound electrons from the continuum to a discrete state or transitions within the atomic and ionic energy continuum. Under optimum discharge conditions, the plasma in the capillary channel is so highly perturbed that the upper energy states of the atoms and ions merge into a continuum. Their lifetime in this perturbed state has been determined from the behavior of the outflowing plasma and is approximately 10^{-8} s.

4. MEASURED AND CALCULATED DEPTHS OF THE CONTINUUM OF ATOMIC AND IONIC UPPER ENERGY STATES

The plasma pressure in the capillary channel was calculated from the mass evaporated by the capillary walls per capacitor discharge, and an average was evaluated over 1 000 discharges. The result was 60 ± 20 atm. The concentration of silicon atoms in the channel was approximately 2×10^{18} cm^{-3} and the concentration of oxygen was 4×10^{18} cm^{-3}. The degree of ionization of oxygen and silicon atoms was determined from the Saha formula,[22] using the nomogram given in Ref. 40. These concentrations were 99.6, 90, and 5% for OI, OII, and OIII, and 99.9, 96.5, 93 and 43% for SiI, SiII, SiIII, and SiIV, respectively. Consequently, the plasma consists mostly of charged particles. The number of neutral atoms of silicon in the plasma is 10^{15} cm^{-3}. The spectral-line emission by atoms of this concentration is readily recorded in arc and spark discharges. However, the radiation emitted by plasma in the capillary channel does not contain these atomic lines, which indicates that the electron configuration of the atoms is highly perturbed to the extent that a continuum of energy states is formed.

For the above concentrations of oxygen and silicon atoms and their degree of ionization, the concentration of electrons in the plasma in the capillary channel is of the order of 5×10^{19} cm^{-3}.

In the highly ionized and dense plasma located in the microfields produced by the ambient ions, the ionization energy of atoms and ions is approximately given by[41]

$$E - E_1 = 6{,}95\cdot 10^{-7} Z_{\rm eff}^{2/3} N_{\rm e}^{1/3}, \tag{4.1}$$

where $N_{\rm e}$ is the concentration of electrons in the plasma. Consequently, an electron bound to a nucleus becomes free once it has received the energy E_1.

The low-frequency fields due to ions and the high-frequency fields due to electrons produce a very considerable perturbation of the unfilled atomic and ionic shells to the extent that the uppermost energy states begin to overlap and form a continuum that, according to the theory in Ref. 32 (which takes into account perturbations by ions) and the theory in Ref. 42 (which takes into account perturbations by electrons) can be approximately determined from[42]

$$E_1 - E_l = \Delta E = 4 Z_{\rm eff}^{4/5} (a_0^3 N_{\rm e})^{4/15} E_{\rm d}, \tag{4.2}$$

where $a_0 = 4\pi\varepsilon_0(\hbar)^2/me^2$, ε_0 is the permittivity of empty space, E_l is the energy of the lowest state in the continuum, and $E_{\rm d}$ is the energy of the lowest discrete level, the transition to which defines the limit of the bright continuum. Consequently, electrons in the unfilled shell of the electron configuration can be bound by the field of the nucleus and can be found in the continuum of states. Their transitions within this continuum or to discrete states $E_{\rm d}$ should be accompanied by a continuous emission.

The results of these calculations are listed in columns 4–9 of Table I in the upper rows for each atom and ion. Columns 10–17 show the calculated values taken from the tables reproduced in Refs. 43 and 44.

Comparison of the numerical values in columns 9, 10, and 12 shows that the discrete character of the ionic resonance lines of magnesium persists as the current density increases, because the upper level lies in each case below the continuum of ionic energy states.

Comparison of the numerical values in columns 9, 10, and 15 shows that the upper level of the atomic resonance lines and the SiIII 254.1-nm line also lies below the continuum calculated from (4.2). However, the resonance lines of

magnesium and silicon atoms are absent against the background of the continuous spectrum, although the concentration of neutral silicon atoms is of the same order of magnitude as the concentration of magnesium ions in the plasma. On the other hand, the concentration of SiIII ions is higher by three orders of magnitude than the concentration of magnesium ions. Despite this, the SiIII 254.1-nm line is not seen against the continuous background because it and the resonance lines of silicon and magnesium atoms are broadened by the increase in the current density until they disappear altogether. This discrepancy between experiment and theory may be due to some error in the derivation of (4.2).

The numerical factor in (4.2) is introduced in order to obtain agreement between the line widths and the average quasistatic profiles, interpolated from the detailed Holtzmark profiles.[45] This may be subject to error in the estimated line width because of the neglect of charged-particle correlations and the fact that certain theoretical difficulties have been ignored.[42] For these reasons, the uncertainty in the shift of the series limit may be as high as 30%. Another possible source of error is that the derivation of (4.2) was based on the assumption that the only perturbing particles were electrons and singly-charged ions.[42] Actually, the plasma under investigation consists mostly of doubly-charged ions and a substantial number of triply-charged ions. Moreover, the perturbing effect of microfields of thermal origin is substantially enhanced in both magnitude and frequency as a result of plasma-density pulsations with the frequency of 3.66 μs^{-1}, which can be seen on the current oscillogram (Fig. 12),[46] and the rapid displacement of the plasma. Consequently, the perturbing effect of the charged plasma particles on the energy states of the radiators is so great that the numerical factor in (4.2) can be doubled. The second row given for each atom in Table I shows the result of calculations in which the numerical factor in (4.2) was increased by a factor of 1.75. The experimental results in the visible and ultraviolet ranges are then in agreement with calculations. Comparison of the calculations listed in column 8 of Table I show that the change in the position of the limit of the series of discrete terms due to the increase in the numerical factor in (4.2) is within the limits of uncertainty in the theory ($\sim 30\%$) for all atoms and ions, with the exception of OIII and SiIV ions for which the shift of the limit is 38% and 36%, respectively.

Consequently, the spectral range above 225 nm is due to electron transitions within the continuum of states and transitions from the continuum to the ground state of atoms, and also electron transitions within the ionic continuum above 55 000, 80 000, 190 000, 180 000, and 260 000 cm^{-1} for SiII, SiIII, SiIV, OII, and OIII, respectively. This explains the formation of a pure continuous spectrum without emission lines superimposed upon it. In the plasma that we have investigated, the continuous spectrum above 225 nm is due to the broadening of the 22 lines of SiI, 17 lines of SiII, 49 lines of SiIII, 29 lines of SiIV, 221 lines of OII and 151 lines of OIII. The radiation emitted by neutral oxygen atoms is confined to wavelengths below 225nm. The numerical values listed in column 7 and the expressions given by (1.7) show that the continuous spectrum is emitted by the above plasma mostly as the result of line broadening.

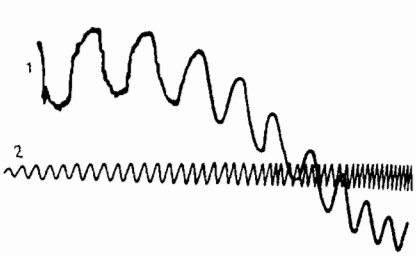

FIG. 12. Current oscillogram recorded with the OK-19M-2 high-voltage oscillograph: *1*—current oscillogram (current pulsation due to pulsation in plasma density), *2*—time scale (one oscillation corresponds to 0.09 μs). The complete oscillogram scan corresponds to 3μs.

The energy distribution in the spectrum depends substantially on whether the spectrum is photographed directly in the capillary channel or after it has passed through the flare produced by the outflowing plasma. The energy was estimated for the plasma in the capillary channel from the relative intensity at 250, 400, and 600 nm, with corrections for plasma temperature, spectrograph dispersion and absorption by quartz. These calculations showed that, when the current was of the order of 10^6 A/cm^2, the continuous emission by the plasma in the capillary channel was thermal in character.

We therefore conclude that, under certain definite conditions in the discharge, the atoms and ions occupy a continuum of upper energy states ΔE, the depth of which can be calculated from (4.2) with acceptable accuracy after the numerical factor has been adjusted and determined experimentally from the vanishing of the lines.

When $\Delta E/kT > 1$ and, even more so, when $\Delta E/kT \gg 1$, the continuous spectrum from the capillary channel is of thermal origin and can be described by Planck's distribution.

The continuous emission that has passed through the peripheral layers (flare) of the inhomogeneous plasma is described by Unsöld's equation (1.8).

When $\Delta E/kT > 1$, the continuous emission is described by Biberman's formulas (9) and (10) (Ref. 28). The effect of inhomogeneity on emitted spectral lines must be taken into account in the case of an optically dense plasma.[47]

[1] Th. Lyman, Astrophys. J. **60**, 1 (1924).
[2] Th. Lyman, Nature (London) **118**, 156 (1924).
[3] J. A. Anderson, Astrophys. J. **75**, 394 (1932).
[4] G. Rathenau, Z. Phys. **87**, 394 (1933).
[5] S. I. Gasilevich, Papers presented at the Leningrad Optics Institute [in Russian], Leningrad, 1934, p. 453.
[6] W. Finkelnburg, Z. Phys. **88**, 297 (1934).
[7] W. Finkelnburg, *ibid.*, p. 763.
[8] W. Finkelnburg, Kontinuierliche Spectren, Berlin, 1938.
[9] L. Wyneken, Ann. Phys. (Leipzig) **86**, 1071 (1928).
[10] W. Elenbaas, Physica **3**, 859 (1935).
[11] W. Elenbaas, *ibid.*, p. 176.
[12] W. Elenbaas, *ibid.*, p. 762.
[13] A. Unsöld, Ann. Phys. (Leipzig) **33**, 607 (1938).
[14] J. A. Gaunt, Proc. R. Soc. London **A126**, 654 (1930).
[15] A. W. Maue, Ann. Phys. (Leipzig) **13**, 161 (1932).
[16] A. A. Babushkin, Thesis [in Russian], Leningrad Optics Institute, 1941.
[17] A. A. Babushkin, Zh. Eksp. Teor. Fiz. **14**, 156 (1944).
[18] A. A. Babushkin, *ibid.*, p. 184.
[19] A. A. Babushkin, *ibid.*, p. 479.
[20] A. A. Babushkin, *ibid.*, **15**, 32 (1945).
[21] B. Yur'ev, *Experimental Aerodynamics* [in Russian], Part 1, 74, 1939.
[22] M. Saha, Philos. Mag. **40**, 472 (1920).
[23] Th. Hahn and W. Finkelnburg, Z. Phys. **122**, 36 (1944).
[24] W. Finkelnburg, J. Opt. Soc. Am. **39**, 185 (1949).

[25] H. Muraour, J. Romand, and B. Vodar, C. R. Acad. Sci. **223**, 620 (1945).
[26] J. Romand and B. Vodar, *ibid.*, **224**, 1634 (1947).
[27] J. Romand and B. Vodar, *ibid.*, **225**, 574.
[28] L. M. Biberman and Norman, Usp. Fiz. Nauk. **91**, 193 (1967) [Sov. Phys. Uspekhi **10**, 52 (1967)].
[29] N. N. Ogurtsova and I. V. Podmoshenskiĭ, Opt. Spektrosk. **4**, 539 (1958).
[30] N. N. Ogurtsova, I. V. Podmoshenskiĭ, and V. M. Schelemina, *ibid.*, **15**, 743 (1963) [Opt. Spectrosc. (USSR) **15**, 404 (1963)].
[31] N. N. Ogurtsova, I. V. Podmoshenskiĭ, and V. M. Schelemina, *ibid.*, **16**, 949 (1964) [*ibid.*, **16**, 514 (1964)].
[32] D. R. Inglis and E. Teller, Astrophys. J. **24**, 355 (1948).
[33] V. N. Egorova, V. I. Isaenko, A. A. Mak, and A. I. Sadykova, Zh. Tekh. Fiz. **32**, 338 (1962) [Sov. Phys. Tech. Phys. **7**, 242 (1962)].
[34] G. V. Ovechkin, Zh. Eksp. Teor. Fiz. **22**, 610 (1952).
[35] G. V. Ovechkin and I. A. Gael, Zh. Prikl. Spektrosk. **12**, 804 (1970) [J. Appl. Spectrosc. (USSR) **12**, 598 (1970)].
[36] G. V. Ovechkin, Uch. Zap. BGU, Ser. fiz.-mat., No. 32 (1957).
[37] G. V. Ovechkin, *ibid.*, No. 41, 105 (1958).
[38] G. V. Ovechkin, *ibid.*, p. 124.
[39] I. I. Levintov, Izv. AN SSSR, Ser. fiz. **11**, 29 (1947).
[40] A. Unsöld, *The Physics of Stellar Atmospheres* [in German], Springer, Berlin, 1955 [Russ. transl. of an earlier ed., IL, M., 1947].
[41] A. Unsöld, Astrophys. J. **24**, 355 (1947).
[42] H. R. Griem, *Plasma Spectroscopy*, McGraw-Hill, N.Y., 1964 [Russ. transl., Atomizdat, M., 1969, p. 355].
[43] W. L. Wiese, M. W. Smith, and B. M. Glennon, *Atomic Transition Probabilities*, U.S. Govt. Printing Office, Washington, D.C., V. 1, 1966.
[44] W. L. Wiese, M. W. Smith, B. M. Glennon, *Atomic Transition Probabilities*, U.S. Govt. Printing Office, Washington, D.C., V. 2, 1969.
[45] A. B. Underhill and J. A. Waddell, U.S. National Bureau of Standards, Circ. 603 (1959).
[46] G. V. Ovechkin and F. H. Bakhtovarshoev, Izv. AN Tadzh. SSSR, Ser. fiz.-mat. nauk, No. 3 (113), 20 (1989).
[47] G. V. Ovechkin, Zh. Prikl. Spektrosk. **24**, 412 (1976) [J. Appl. Spectrosc. (USSR) **24**, 284 (1976)].

Translated by S. Chomet